IEEE Access
Multidisciplinary ⋮ Rapid Review ⋮ Open Access Journal

Received 21 December 2023, accepted 3 January 2024, date of publication 11 January 2024, date of current version 22 January 2024.

Digital Object Identifier 10.1109/ACCESS.2024.3352911

RESEARCH ARTICLE

Asymmetric Bimanual ADL Training With Underactuated Exoskeleton Using Independent Joint Control and Visual Guidance

THOMAS M. KWOK[1], (Member, IEEE), AND HAOYONG YU[2], (Senior Member, IEEE)
[1]Integrative Sciences and Engineering Programme, NUS Graduate School, National University of Singapore, Singapore 117575
[2]Department of Biomedical Engineering, National University of Singapore, Singapore 117575

Corresponding author: Thomas M. Kwok (thomasm.kwok@u.nus.edu)

This work involved human subjects or animals in its research. Approval of all ethical and experimental procedures and protocols was granted by the National University of Singapore Institutional Review Board.

ABSTRACT This paper addresses the challenges in existing upper limb robotic rehabilitation training for asymmetric bimanual activities of daily living (ADL), crucial for stroke patients' ADL-related functional recovery. Our proposed exoskeleton control framework introduces independent joint control and visual guidance in virtual reality (VR) to facilitate asymmetric bimanual ADL training. Unlike conventional task-space control methods, our approach implements independent joint control into underactuated exoskeletons, offering individualized assistance tailored to patients' joint impairment conditions. The framework utilizes human-demonstrated ADL motions for joint trajectory planning, potentially teaching compensatory techniques with unique joint coordination patterns through therapist demonstrations. To address interjoint coordination challenges in underactuated exoskeletons, VR visual guidance aids patients in self-coordinating unassisted and assisted joints. The proposed framework was evaluated by human experiments with 15 healthy subjects. It demonstrated the effectiveness of the proposed visual guidance, exhibiting a motion period similar to human-demonstrated motion and statistically significant reductions in angle errors at the shoulder (sF/E-A) and wrist (wF/E-A). The robot assistance provided by the control framework was further validated through statistically significant reductions in electromyography (EMG) and angle errors at robot-assisted joints. This proof-of-concept on healthy subjects suggests the potential of our control framework to assist stroke patients in asymmetric bimanual ADL training.

INDEX TERMS Upper limb exoskeleton, stroke rehabilitation, asymmetric bimanual ADL training, joint-space control, virtual reality.

I. INTRODUCTION

Upper limb motor function impairment is prevalent among stroke patients and affects them significantly; some patients reported it as one of the most distressing sequelae [1]. Around 80% of stroke populations have upper limb motor function impairment [1]; the impaired motor functions affect their activities of daily living (ADL), thus influencing their social re-integration [2]. With advanced robotic technology, exoskeletons can provide repetitive and consistent rehabilitation training with joint-by-joint assistance for patients to improve motor function without burdening healthcare professionals.

Asymmetric bimanual ADL training is often overlooked but necessary for stroke patients to regain ADL-related functions. The current robotic training focusing mainly on symmetric bilateral arm motion [3], [4], [5] is insufficient to train interlimb coordination because patients may have difficulties

The associate editor coordinating the review of this manuscript and approving it for publication was Giacinto Barresi.

in in-phase, antiphase, and bilateral complementary motion [6], [7]. So, training asymmetric bilateral arm motion is necessary, particularly for the complementary bilateral movement. This dominates ADL [3], [6], like pouring water and cutting bread. Also, patients can train their arm coordination and compensatory technique [8] in asymmetric bimanual ADL training. Yet, limited rehabilitation robotic research focuses on asymmetric bimanual training.

The existing exoskeleton control methods are challenging for asymmetric bimanual ADL training because most are based on task space. Although understanding the target movement in task space is straightforward for patients, providing task-space assistance in post-stroke ADL training is unnecessarily challenging because of (i) stroke patients' joints with different impairment conditions, (ii) specific joint trajectories and coordination when teaching compensatory techniques, and (iii) required motion errors for motor learning.

First, the task-space control framework is challenging to control individual joint assistance, leading to insufficient assistance for severely impaired joints or undesired resistance to less-impaired joints. For example, adjusting robot assistance for different individual joints with task-space impedance control [9], [10], [11] may be difficult. Besides, some research attempting to control individual joint assistance, like the inverse kinematics (IK) method with joint coordination constraints [12], has difficulty assigning joint constraints for specific joint coordination patterns in different ADL tasks.

Second, task-space control is problematic when teaching compensatory techniques in occupational therapy [8]. Those techniques help patients use their remaining abilities to maximize ADL independence. But they require specific joint coordination patterns. Due to different patients' arm lengths and arm redundancy, the exoskeleton with task-space control can assist patients in tracking preset task-space trajectories with many combinations of joint trajectories; their inter-joint coordination may differ from the preset trajectory. So, therapists cannot teach patients compensatory techniques with specific joint coordination patterns in robotic therapy.

Third, some task-space control focused on correcting patients' motion errors. For instance, the joint position control with IK [12], [13], [14] and the task-space adaptive control, like the Barrier composite energy function scheme [19], followed the preset task-space trajectories by accurately tracking generated joint trajectories. However, this provides insufficient motion error in both task and joint space for motor learning [15]. Also, it may demotivate patients and lead to patient-passive training, affecting training outcomes [16].

We understand that tracking task-space trajectory can guarantee ADL task success and patients' safety, but it is unnecessary if the task is performed in virtual reality (VR). VR can guarantee patients' safety when they fail the ADL task. For example, no actual harm is done to patients when dropping the utensil in the VR food preparation task. Also, motion error and task failure enhance motor learning, favoring recovery progress.

Hence, joint-space control may be a promising alternative for robot assistance in VR ADL training since humans can also plan and perform joint-space movement [17]. The advantages of joint-space control include individually assisting less-impaired and impaired joints with different levels of robot assistance. As well as it can be applied in not only redundantly-actuated exoskeletons like Harmony [18] and ARMin [19] as task-space control does, but also underactuated exoskeletons with passive joints like ASSISTON-SE [20] and NESM [21]. These underactuated exoskeletons challenge robot control due to the combination of active and passive joints; limited existing control frameworks were suitable for underactuated exoskeletons assisting patients in ADL. Yet, joint-space control has two main technical challenges in joint trajectory and coordination.

One of the challenges is finding joint reference trajectories in ADL tasks, which are necessary for robot joint controllers like impedance [21] and assist-as-needed control [22], [23]. The reference movements are difficult to define since human arm redundancy allows therapists/patients to perform ADL tasks differently. Let alone various interlimb coordination patterns for complementary bilateral movements and the patient-specific compensatory technique. Although the reference trajectories can be defined by therapists [10] or robot developers [22], the preset joint reference may not help patients perform ADL tasks because they have different arm lengths. With forward kinematics, we can expect that their hand trajectories are significantly affected by arm lengths, even with the same joint trajectory. Also, patients confused by the preset arm movements would most likely act against the robot's assistance, affecting their motor learning progress.

Another issue for joint-space control is the coordination between assisted and unassisted joints. The impaired joint assisted by exoskeletons may not coordinate with those unassisted joints freely mobilized by patients because they do not know the robot motion regarding motion timing and joint angle. Such uncoordinated motions may confuse and demotivate patients during ADL training.

So, this paper demonstrates a novel control framework to address the mentioned challenges in task-space assistance, joint trajectory planning, and coordination with unassisted joints. The control framework combines independent joint control and VR visual guidance, aiming to support asymmetric bimanual ADL training and assist patients with therapist-demonstrated joint trajectories. Independent joint control with impedance control and robot weight compensation assists individual impaired joints, allowing joint motion error for motor learning and balancing the robot weight. Real-time VR visual guidance helps patients in self-coordinating unassisted and assisted joints. It aids subjects in anticipating robot assistance from active joints and matching with their unassisted joint motion. Also, in VR, therapists and patients can share the same virtual arm to record and train arm

movement; patients with different arm lengths can use recorded joint motions to train ADL skills.

The rest of the paper is organized as follows. Section II describes the exoskeleton used for implementation and the proposed control framework. Sections III and IV present the experimental results of joint controller performance and robot assistance in an ADL task with 15 healthy subjects. Finally, Section V contains a discussion and potential research contributions.

II. METHODS

To solve the mentioned challenges in asymmetric bimanual ADL training, this paper proposed a new control framework using independent joint control and visual guidance in VR with three novelties:

1) Apply joint-space control instead of task-space control in asymmetric bimanual ADL training, providing individual assistance for impaired joints.

2) Use the same virtual arm in VR to record human-demonstrated joint motions and teach patients. This solves the joint reference trajectory and arm length issues, outlining the possibility of providing compensatory techniques for ADL training in occupational therapy.

3) Show patients real-time VR visual guidance, guiding them to follow the demonstrated joint motions and coordinate their unassisted and assisted joints.

However, unlike task-space control, this control framework cannot guarantee ADL task success because of passive/unassisted joints mobilized by patients. So, we will study the effect of visual guidance and individual joint assistance in the proposed control framework in the following sections.

A. UNDERACTUATED UPPER LIMB EXOSKELETON (UULE)

To show the potential of the proposed control in underactuated exoskeletons, we implemented the control in the Underactuated Upper Limb Exoskeleton (UULE) [24]. This is a bilateral underactuated exoskeleton that assists chronic stroke patients in bimanual ADL training, as shown in Fig. 1. From Hu's work [25], we understand that many chronic stroke patients' proximal motor function has been improved after intensive training in the early stage of stroke. So, UULE aims to provide joint-space assistance from elbow to hand for impaired distal joints while conforming with less-impaired scapula/shoulder joint motions.

In this paper, the proposed control framework was implemented into UULE's four active joints for evaluating the robot assistance in shoulder flexion/extension (sF/E-A, q_4), elbow flexion/extension (eF/E-A, q_6), forearm pronation/supination (eR-A, q_7), and wrist flexion/extension (wF/E-A, q_8). With the passive mechanism (ball joint and circular guide), UULE cannot assist but conform to patients' scapula protraction/retraction (sP/R-P, q_1, q_2, q_3) and shoulder internal/external rotation (sR-P, q_5). Furthermore, such passive joints can represent robot joints under the transparent mode (without assistance) in redundantly actuated exoskeletons.

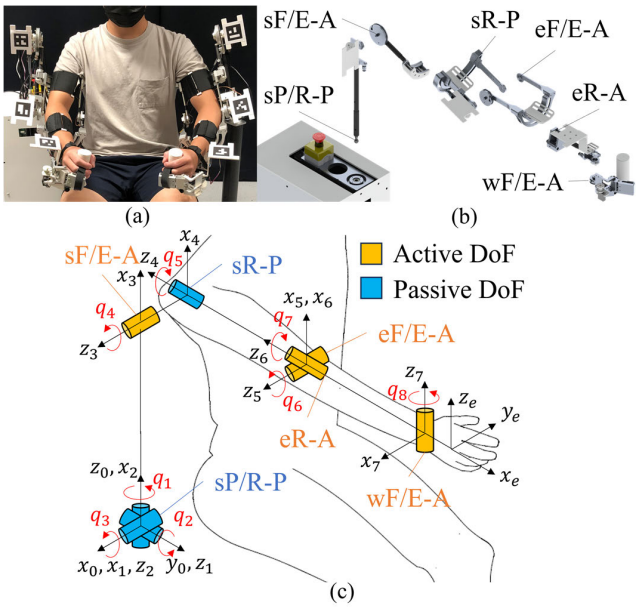

FIGURE 1. (a) UULE design, (b) exploded diagram and (c) kinematics.

Hence, the experimental results are applicable for redundantly actuated and underactuated exoskeletons.

As to actuation, each active joint was connected to a linear series elastic actuator (SEA) with a pair of Bowden cables. The sF/E-A and three other joints (eF/E-A, eR-A, and wF/E-A) used springs with a stiffness of 56.62 N/mm and 16.34 N/mm, providing maximum cable forces of 707.75 N and 318.63 N with bandwidths of 64.8 Hz and 35.0 Hz. These active joints are sufficient to assist patients' motions during ADL training according to the requirements of joint torque [26] and bandwidth (1-10 Hz) [27].

Regarding exoskeleton sensing feedback for controller and VR, joint kinematics were measured by absolute rotary encoders and visual-inertial sensors. The encoders measured hinge joint angles (sF/E-A, eF/E-A, and wF/E-A), while visual-inertial sensors measured ball and revolute joint angles (sP/R-P, sR-P, and eR-A). More details can be found in our previous works [24].

Additionally, UULE, configured bilaterally, facilitates bimanual training. Despite its capacity to assist both arms, our focus is on patients with one impaired arm, a common scenario in stroke cases [28]. To validate the effectiveness of our control framework in our proof-of-concept experiments (Section III), we assisted the subjects' right arm with four actuated joints, given its involvement in more intricate movements (i.e., steak cutting motion) than the left arm (i.e., steak holding motion). So, in the experiment, UULE exclusively assisted the right arm, leaving all left-side joints unactuated.

B. INDEPENDENT JOINT CONTROL WITH VISUAL GUIDANCE

We propose a novel control framework that combines independent joint control and VR visual guidance to provide

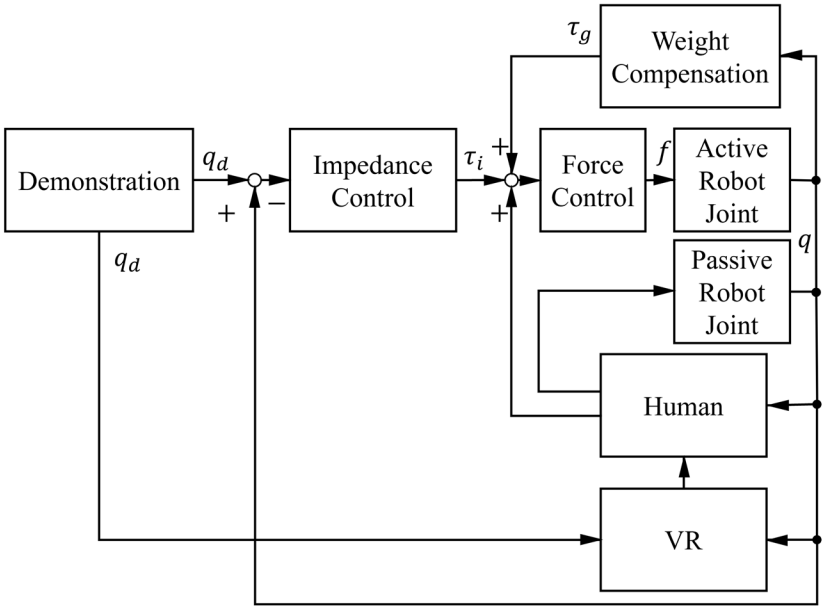

FIGURE 2. The control framework with independent joint control and VR visual guidance.

asymmetric bimanual ADL training. According to therapists' demonstrated joint trajectories, independent joint control can individually assist patients with impaired joints. At the same time, real-time visual guidance in VR can visually guide patients to coordinate their less-assisted/unassisted joints with robot-assisted joints in terms of motion timing and joint angle.

The detailed control framework is depicted in Fig. 2. Initially, a therapist wears UULE and demonstrates the arm motion tailored to the patient's residual movement capabilities in a VR ADL task. Concurrently, UULE records the therapist's joint movements, establishing reference trajectories for joint impedance controllers and providing real-time visual guidance. Subsequently, the patient is assisted by active joints of UULE and guided by visual guidance showing reference trajectories for assisted and less-assisted/unassisted joints. With the patient's motion captured by UULE and displayed in VR, the patient compares his/her arm motion with visual guidance (i.e., a guiding arm with the same dimension as the patient's virtual arm in VR). The patient then anticipates robot motion of assisted joints and self-corrects his/her joint motion error at the unassisted joints to align with visual guidance. Based on the patient's performance observed in VR, the therapist can adjust the demonstrated motion in the subsequent trial, ensuring a personalized and adaptive rehabilitation process.

Although the therapist-demonstrated trajectory may address the joint trajectory planning issue in exoskeletons, the joint trajectories and the guiding arm may not be intuitive enough to patients, causing them confusion and resisting the robot's assistance. Hence, the experiment in Section III is essential to study the human response to robot assistance and visual guidance under the proposed framework.

1) INDEPENDENT JOINT CONTROL

The UULE applies independent joint control for four active joints. Each joint has two control layers: (i) a low-level force control for SEA and (ii) a high-level control for impedance control and robot weight compensation. The detailed control block diagram is shown in Fig. 3.

Since linear SEAs actuated active joints via cables, a low-level control layer was implemented to control the output cable force of SEA for robot joint actuation. This layer was achieved by a proportional derivative (PD) force controller, tracking the desired cable force (f_d) commanded by the high-level control layer. The tracking force error (e_f) between desired cable force (f_d) and the force feedback measured by SEA (f) was fed back to the PD force controller, and the current command for motors was computed with control gains of force controller (proportional (K_f) and derivative terms (D_f)). These control gains were tuned empirically to achieve a satisfying force-tracking performance.

On the high-level control layer, the UULE applied impedance control and robot weight compensation. The desired joint torques, i.e., cross products of the moment arm of active joints (r) and desired cable forces (f_d), are the joint torque summation of impedance control (τ_i) and robot weight compensation algorithm (τ_g).

In the impedance controller, the torque command (τ_i) was computed by (1) with the robot joint feedback (q, *dot (q)* and therapist-demonstrated joint trajectories (q_d, $\dot{q_d}$):

$$\tau_i = K e_q + D \dot{e_q}, \tag{1}$$

where $e_q = q_d - q$, $\dot{e_q} = \dot{q_d} - \dot{q}$. Also, K and D are proportional (virtual stiffness) and derivative (virtual damping) gains of impedance control. Therapists can customize the robot assistance with these control gains to meet

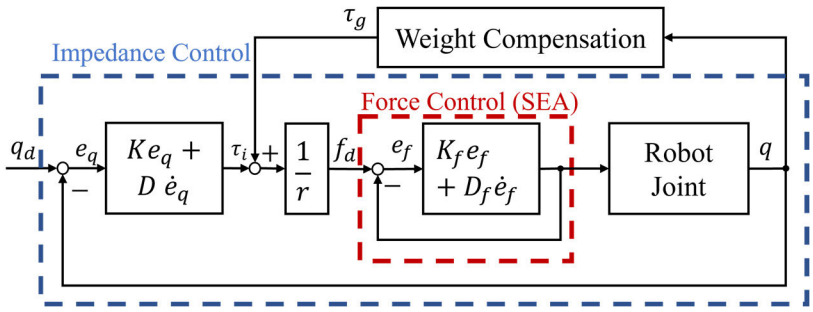

FIGURE 3. The detailed control block diagram for each active joint.

rehabilitation training needs. For example, increasing the K gain enhances robot assistance and minimizes allowable joint motion error for impaired joints. Conversely, therapists can enable the transparent mode for joint compliance, particularly at less-impaired joints, by setting control gains (K, D) to zero. This customization through impedance control permits joint motion errors that foster patients' motor learning [15],while maintaining a safe interaction force range between patients and the exoskeleton.

To mitigate the influence of robot weight on impedance controllers, we have implemented robot weight compensation to minimize the motion bias introduced by the robot weight during patient training. The robot weight compensation provides additional torque (τ_g) to the impedance controller (τ_i) at the high-level control layer. Such additional torque can be estimated by the UULE's model with the Lagrange-Euler equation [29] and joint angle feedback (q), shown in (2)-(4).

$$\tau_{g,i} = \frac{\partial P}{\partial q_i} = \sum_{j=i}^{n} -m_j g^T u_{ji} \bar{r}_j^j, \tag{2}$$

where p is the total potential energy of the robot, u_{ji} term and homogeneous transformation matrix (T_i^{i-1}) are

$$u_{ji} = \frac{\partial T_j^0}{\partial q_i} = T_{i-1}^0 Q_i T_j^{i-1} \tag{3}$$

$$T_i^{i-1} = \begin{bmatrix} cq_i & -c\alpha_i sq_i & s\alpha_i sq_i & a_i cq_i \\ sq_i & c\alpha_i cq_i & -s\alpha_i cq_i & a_i sq_i \\ 0 & s\alpha_i & c\alpha_i & d_i \\ 0 & 0 & 0 & 1 \end{bmatrix} \tag{4}$$

In terms of impedance control and robot weight compensation, UULE does not offer robot assistance at passive joints (i.e., sP/R-P and sR-P). However, considering UULE's design for patients with less-impaired proximal joints, we believe this limitation should not be a significant concern.

2) VISUAL GUIDANCE AND FEEDBACK IN VR

As mentioned above, the visual guidance and feedback in VR were represented as connected virtual arms, as shown in the guiding arm ③ and virtual arms ①, ② in Fig. 4. The existing literature has three VR representations for an arm: a connected virtual arm, a detached virtual arm, and

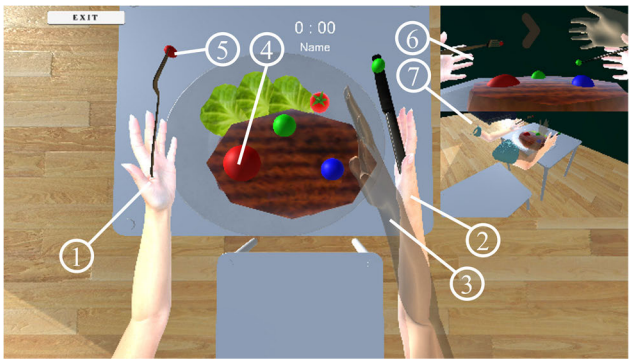

FIGURE 4. The independent joint control with VR visual guidance. The figure shows ① the unassisted arm, ② assisted arm, ③ a guiding arm as visual guidance, ④ targets (red, green, and blue) for utensils, ⑤ the contact point of the fork, ⑥ the back view, ⑦ the isometric view.

virtual objects. In this paper, we chose a connected virtual arm to represent the visual guidance and feedback because it can simultaneously show patients multi-joint and hand movements in both joint and task spaces. This is essential when patients coordinate their unassisted joints and assisted joints. Additionally, such connected virtual arms can develop patients' body ownership [30] due to the similar look to their real arms, while the detached virtual arm and virtual objects may negatively affect their body ownership and arms control in VR, slowing the training progress, as suggested in [31].

Regarding virtual arm motion, the guiding arm was updated by Forward Kinematics (FK) in Unity3D with therapist-demonstrated joint trajectories, while the patient's virtual arm was updated with robot joint feedback (q). Further, the translations of guiding and virtual arms can be achieved by the therapist's and patient's shoulder translations, estimated by the passive ball joint at sP/R-P and a long radius between sF/E-A and sP/R-P. More details on the kinematic model of virtual arms can be found in our previous work [24].

Furthermore, the same connected virtual arm was used for therapists to demonstrate the ADL motion and for patients to use as visual guidance and feedback. Due to different arm lengths and redundancy, the therapist's and patient's joint trajectories may differ when completing the same ADL task, even with the same task-space trajectory. Also, it would be

challenging for patients to follow guiding arms at different lengths during training. Hence, the same connected virtual arm was used for therapist demonstration, patient guidance, and feedback. Then, the therapist-demonstrated trajectories can be applied to patients without concern about the arm length issue.

3) VR ADL TASK

As to the ADL task, the steak-cutting task, one of the feeding tasks for eating with utensils [32], was selected in this paper, although the proposed control framework is suitable for other asymmetric bimanual ADL tasks. Furthermore, the steak-cutting task was held in VR due to visual guidance and patient safety. Besides, we used non-immersive VR (displayed on monitors) in this paper to demonstrate the effectiveness of the proposed control framework, but we believe that immersive VR [33] should achieve a similar VR effect on patients.

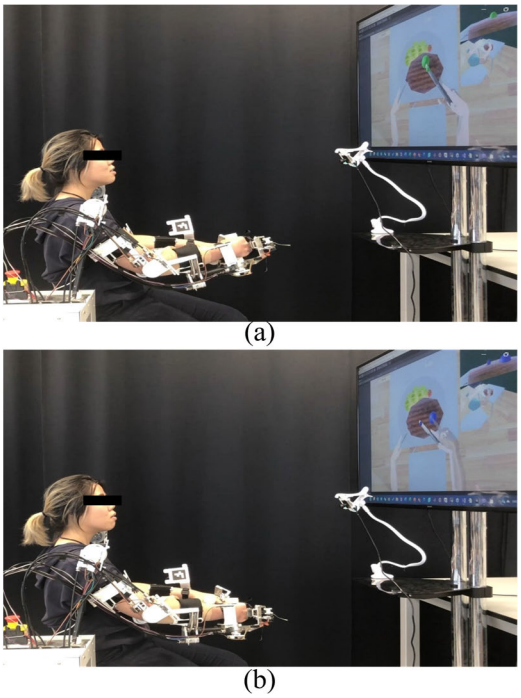

FIGURE 5. The subject (a) held the virtual knife and approached the green target during the forward cutting motion (for three times), (b) and approached the blue target during the backward cutting motion (for twice).

In this VR steak-cutting task shown in Fig. 4, patients were required to perform an asymmetric bilateral complementary motion. Their left arm held the steak down by touching and disabled the red target ④ with the red contact point of the fork ⑤, while their right arm cut the steak by touching the green and blue with the same colored contact point of the knife. Specifically, patients touched and disabled the green target with a knife during the forward cutting motion and the blue target during the backward motion, shown in Fig. 5. Furthermore, the patient's motion, i.e., unassisted arm ①, assisted arm ②, and guiding arm ③ in Fig. 4, were updated with the real-time sensing feedback from UULE. To guarantee bimanual motion in this task, the guiding arm replayed the demonstrated motion only when the red target ④ was disabled.

Additionally, as shown in Fig. 4, three views were displayed for patients to comprehend the task scene, including the top view as the main view, back view ⑥, and isometric view ⑦.

III. EXPERIMENTS

A. SYSTEM HARDWARE

The sensors and controller of UULE were implemented in the PC/104, a Linux system with the real-time kernel patch (RT-Preempt).

As for sensors, absolute rotary encoders and visual-inertial sensors were used in UULE. Three encoders (Renishaw RLS, RM08) measured angles of sF/E-A, eF/E-A, and wF/E-A at 500 Hz, while three visual-inertial sensors measured that of sP/R-P, sR-P, and eR-A at 100 Hz. As shown in Fig. 1, each visual-inertial sensor consisted of an Aruco marker (5cm x 5cm) and a customized inertial measurement unit (IMU) with a chip (BNO080, Bose, US). The marker's orientation measurement, fused 10 Hz camera feedback (720 p/120 fps) and 100 Hz IMU data, was sent to the PC/104 for joint angle calculations. More details and the experimental validation of sensors in the VR ADL task can be found in [24]. Subsequently, joint angle measurements were sent to Unity3D in another computer through User Datagram Protocol (UDP) at 70 Hz with 2.983ms of connection latency. Simultaneously, these measurements were sent to PC/104 as angle feedback for independent joint controllers and robot weight compensation.

When the impedance controller tracked joint reference trajectories with the angle feedback at 300 Hz, combined with robot weight compensation, it generated force commands for SEAs. Then, SEA force controllers tracked force commands by sending the current commands to motors (MYACTUATOR, RMD-L-5010 10T). The force feedback for the SEA controller was estimated by springs and linear encoders (Renishaw RLMD01_08).

B. CHARACTERIZATION OF JOINT IMPEDANCE CONTROLLER

To provide robot assistance, each active (cable-driven) joint of UULE has implemented an impedance controller. The experiments demonstrate the impedance controller's high fidelity in stiffness control, assisting in the healthy subject experiment with the set stiffness ($\boldsymbol{K_{set}}$). For instance, as illustrated in Fig. 6, the estimated stiffness of impedance controller at eF/E-A is found to be $\boldsymbol{K = 4.190\ Nm/rad}$ through the linear regression between torque feedback and angle. This closely aligns with the set stiffness values ($\boldsymbol{K_{set} = 4.297\ Nm/rad}$). Notably, the estimated stiffness was obtained from three repetitions of pulling eF/E-A back

TABLE 1. Stiffness control responses of all active joints.

Joint	K_{set} (Nm/rad)	K (Nm/rad)	MAE of Linear Regression
sF/E-A	6.818	7.361	0.323
eF/E-A	4.297	4.190	0.160
eR-A	5.013	4.927	0.162
wF/E-A	0.458	0.517	0.174

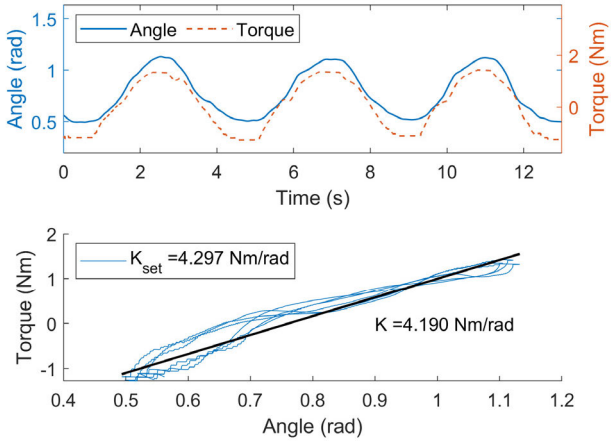

FIGURE 6. Stiffness control responses for eF/E-A ($K_{set} = 4.297\ Nm/rad$, $D_{set} = 0.143\ Nm{\cdot}s/rad$).

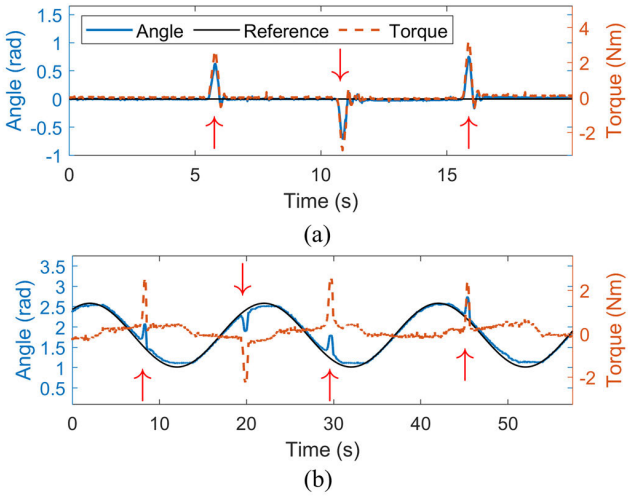

FIGURE 7. The impedance control performance for eF/E-A ($K_{set} = 4.297\ Nm/rad$, $D_{set} = 0.143\ Nm{\cdot}s/rad$) and its response to external disturbances, when (a) tracking a fixed reference point ($q_d = 0$), and (b) a sinusoidal reference trajectory. The red arrows indicate the time when external disturbances are applied.

and forth, resulting in a small mean absolute error (MAE) of 0.160 Nm. Similar experimental results were observed across other active joints, as summarized in TABLE 1.

An additional experiment was conducted to assess the effectiveness of impedance control and compliance behaviors in response to an external disturbance, such as pulling, as indicated by red arrows. The results reveal that the eF/E-A maintained a fixed reference angle (Fig. 7 (a)) and tracked the sinusoidal reference trajectory with an acceptable tracking error (Fig. 7 (b)), even in the presence of external disturbances. So, the impedance controller can track joint reference trajectory and assist patients with the preset robot assistance, i.e., the set stiffness (K_{set}), during rehabilitation training.

C. HEALTHY SUBJECTS EXPERIMENTS

The evaluation of the UULE in an asymmetric bimanual ADL task was conducted on 15 healthy subjects (9 females and 6 males, ages 21-45) who were staff or students at the university. All participants provided informed consent before participating in the experiment, and the protocols were approved by the National University of Singapore Institutional Review Board under approval No. NUS-IRB-2022-337 on September 13, 2022.

In order to verify the effectiveness of the proposed framework consisting of independent joint control and VR visual guidance, the experiment aims to test three hypotheses: (i) a guiding arm as visual guidance can guide subjects; (ii) the proposed framework can assist subjects' one specific joint in asymmetric bimanual ADL task; and (iii) the proposed framework can assist multiple joints simultaneously in an asymmetric bimanual ADL task.

Two experiments can prove these hypotheses. First, compare subjects' motion periods and joint angle errors with and without the guiding arm, while motion periods similar to reference motion and smaller errors are expected in the condition with the guiding arm. Second, compare subjects' electromyography (EMG) and joint angle errors in three operating modes: a transparent mode (no assistance), elbow assistance mode (with actuated eF/E-A only), and arm assistance mode (with actuated sF/E-A, eF/E-A, eR-A, and wF/E-A). Reductions in EMG signals and joint angle errors are expected in those robot-assisted joints. However, since the elbow assistance mode assists subjects' elbow specifically, no significant change is expected in EMG signals and joint angle errors for other unassisted joints like sF/E-A, wF/E-A, and eR-A.

Besides, due to the underactuated mechanism of UULE, uncoordinated movements between assisted and unassisted joints may occur during experiments. This can be observed by larger hand trajectory errors and EMG signals compared to transparent mode.

As mentioned, the steak-cutting task was selected in this experiment. The experiment setup is shown in Fig. 8. In the experiment, subjects were asked to perform a VR steak-cutting task with the UULE ① while their motion was cap-

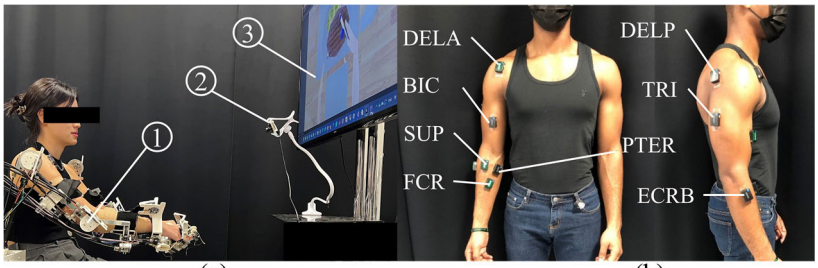

FIGURE 8. (a) Experiment setup for the steak-cutting task, with ① UULE, ② camera, ③ monitor for VR. (b) EMG placement on a subject.

tured by camera ②, IMU, and rotary encoder. At the same time, the visual guidance and feedback were shown in VR on the monitor ③. During the experiment, eight EMG sensors were placed on subjects' right arm to evaluate the robot-assisted joints.

Regarding the experiment protocol, subjects were required to touch five targets (three green and two blue), which appeared individually, to complete the task in one trial. For both experiments, three trials were taken in each experimental condition. Those conditions were (i) with and (ii) without a guiding arm (visual guidance) while operating UULE in transparent mode for Experiment 1; given a guiding arm, operating UULE in (i) transparent mode (no assistance), (ii) elbow assistance mode, and (iii) arm assistance mode for Experiment 2. In the transparent mode, the UULE did not assist subjects but merely complied with their motion, while the elbow and arm assistance modes assisted their elbow and four joints (i.e., shoulder, elbow, forearm, and wrist), respectively.

As mentioned, the assistance modes were achieved by robot weight compensation and independent joint impedance control according to the human-demonstrated joint trajectories. As to control gains of independent joint impedance controllers in both elbow and arm assistance modes, we applied a high $\boldsymbol{K}_{set}$ to accentuate the robot-assisting effect on healthy subjects. The control gains, $\boldsymbol{K}_{set}$, were presented in TABLE 1. Before each experiment session, every subject was given a 10-minute warm-up period with UULE. During this period, we fine-tuned the control gain for each subject to closely align with the mentioned high control gain, while ensuring their comfort and safety. Notably, the controller exhibited no instability issues or significant vibrations throughout experiments, ensuring a smooth and safe testing environment.

Furthermore, subjects were shown the human-demonstrated joint trajectories for impedance controllers as a VR guiding arm. Those trajectories were pre-recorded by one of the authors in the same VR ADL task before the experiment. The same trajectories were applied for all 15 subjects to eliminate the effect of different reference trajectories on subjects.

Besides, the VR task can guarantee bimanual motion and subjects' safety. The guiding arm replays the reference joint trajectories only when the red target in Fig. 4 is disabled; otherwise, the guiding arm stops. This can ensure that subjects perform asymmetric bilateral complementary motion during experiments. Also, subjects can stop the guiding arm and robot assistance by not touching the red target when they feel uncomfortable during the experiment, ensuring their safety. Yet, this safety feature was not activated during the experiment because all 15 subjects could maintain asymmetric motion without stopping the guiding arm.

Apart from the encoder and visual-inertial sensors in UULE for kinematic measurements, eight EMG sensors (Delsys Trigno Avanti Sensor, sampling rate of 2150 Hz) were placed on the subject's right arm to measure the EMG signal, as shown in Fig. 8(b).

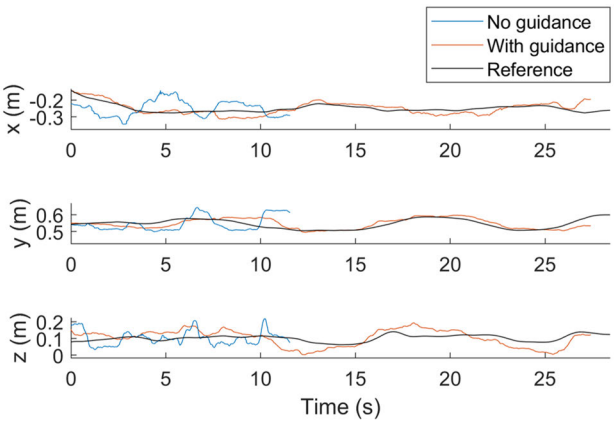

FIGURE 9. Subject J's right virtual hand position in the last trial under transparent mode, with and without visual guidance.

TABLE 2. Relationship between motion, muscles, and EMG sensors.

Motion of joint	Muscle	EMG
Shoulder flexion	Anterior deltoid	DELA
Shoulder extension	Posterior deltoid	DELP
Elbow flexion	Biceps	BIC
Elbow extension	Triceps	TRI
Forearm pronation	Pronator teres	PTER
Forearm supination	Supinator	SUP
Wrist flexion	Flexor carpi radialis	FCR
Wrist extension	Extensor carpi radialis brevis	ECRB

TABLE 2 shows the relationship between joint motions, muscles, and the EMG sensors. EMG signals from each

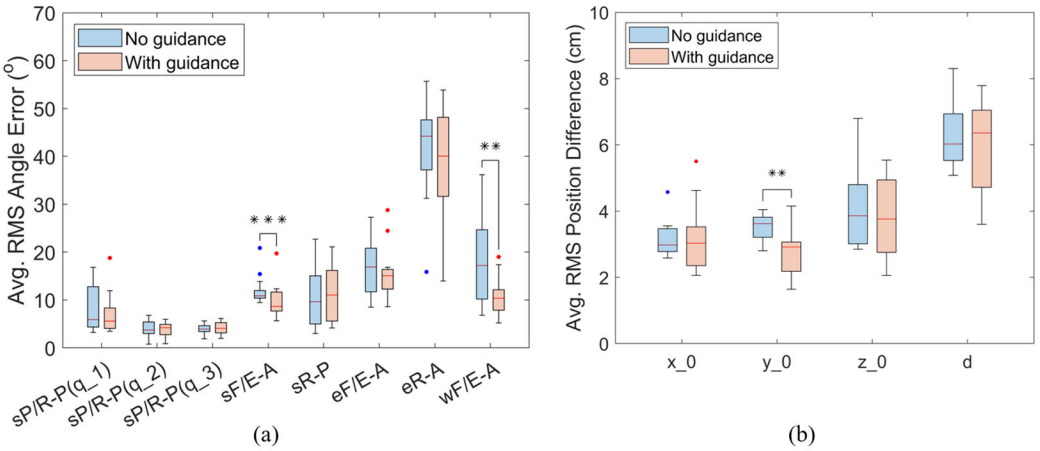

FIGURE 10. Comparison of (a) average RMS joint angle error, and (b) average RMS position difference for right virtual hand with and without visual guidance when no robot assistance is given. The "d" represents Euclidean distance between the virtual hand and guiding hand, and the asterisks ('**,' '***') indicate statistical significance with $p \leq 0.01$, and $p \leq 0.001$ in one-tailed Wilcoxon signed rank test.

sensor have been (i) filtered with a second-order bandpass Butterworth filter with bandwidth 6-800 Hz, (ii) detrended and rectified, (iii) smoothened with the moving average with a window size of 0.2 s, and (iv) normalized to subjects' maximum voluntary contraction (MVC) taken before experiments.

As for data analysis, non-parametric analysis (one-tailed Wilcoxon signed-rank test) was used to analyze the average EMG signals and RMS angle errors across different subjects. This was because the data violated the assumption of normality due to the limited number of subjects. Besides, the outliers were defined as data points lying outside 1.5 times the interquartile range (IQR) above the 75th percentile and below the 25th percentile.

IV. RESULT

Experiment 1 illustrates the effect of visual guidance when completing the VR steak-cutting task, where subjects' motion period and task-space motion resemble the reference motion. Notably, statistically significant reductions in joint angle errors are observed at sF/E-A and wF/E-A. During the experiment, subjects performed the task with and without the guiding arm to verify its effect. As shown in Fig. 9, with visual guidance, the subjects' motion period (27.4 s) and task-space motion were comparable to the reference motion (28.4 s), contrasting with a much shorter period (11.6 s) without guidance. And this observation was consistent with the other 14 subjects.

To evaluate the effect of visual guidance on joint motion patterns, we computed average RMS joint angle errors after synchronizing motions with and without guidance. Fig. 10(a) presents the average RMS joint angle errors in three trials with 15 subjects. The figure shows that the guiding effect is less pronounced in joint motion patterns. Only sF/E-A ($e_q = 2.2°$, $p \leq 0.001$) and wF/E-A ($e_q = 6.8°$, $p \leq 0.01$) exhibit statistically significant error reductions, given their more extensive range of motion. Other joints like sP/R-P (q_1), eF/E-A, and eR-A, merely experience statistically insignificant reductions ($0.3° < e_q < 4.2°$, $0.1 < p < 0.2$). Also, the median of average RMS errors at sP/R-P (q_2, q_3) and sR-P had small and statistically insignificant increases ($e_q < 1.4°$, $p > 0.2$).

Moreover, the observed statistically insignificant reductions ($p = 0.1$) at sP/R-P (q_1) may be attributed to the limited joint motion involved in the steak-cutting task. Regarding eF/E-A, the insignificant reductions ($p = 0.2$) may suggest that subjects did not necessarily require visual guidance for task completion, as the green and blue targets for the knife (Fig. 4) could suffice to guide the elbow angle. Also, outliers at eF/E-A and sP/R-P (q_1) raise the possibility that a few subjects might prioritize specific joints, such as sF/E-A, potentially at the expense of others when following the guiding arm. However, this concern may be insignificant, as this behavior did not result in task failure during the experiments.

Additionally, the statistically insignificant increased RMS angle errors (1.4°) at sR-P and large error at eR-A in Fig. 10(a) may raise a limitation of the guiding arm. Subjects may find it difficult to follow the rotation along the longitudinal axis of the cylindrical arm segments (i.e., upper arm and forearm) in VR. Hence, an additional hand orientation condition for disabling the colored targets should be considered when developing VR steak-cutting tasks, so subjects can complete the VR task with a specific hand orientation.

Besides, Fig. 10(b) presents the average RMS position difference in x-, y-, and z-direction and Euclidean distance (d) between the virtual and guiding hand. The statistically significant reduced position differences in the y-direction and the reduced maximum difference in Euclidean distance indicate that subjects could complete the ADL task with a hand (task-space) trajectory similar to the reference motion when following the guidance. Also, the effect of visual guidance can be observed in Fig. 11 with subject J's right-hand position during the ADL task. Hence, the results suggest that visual

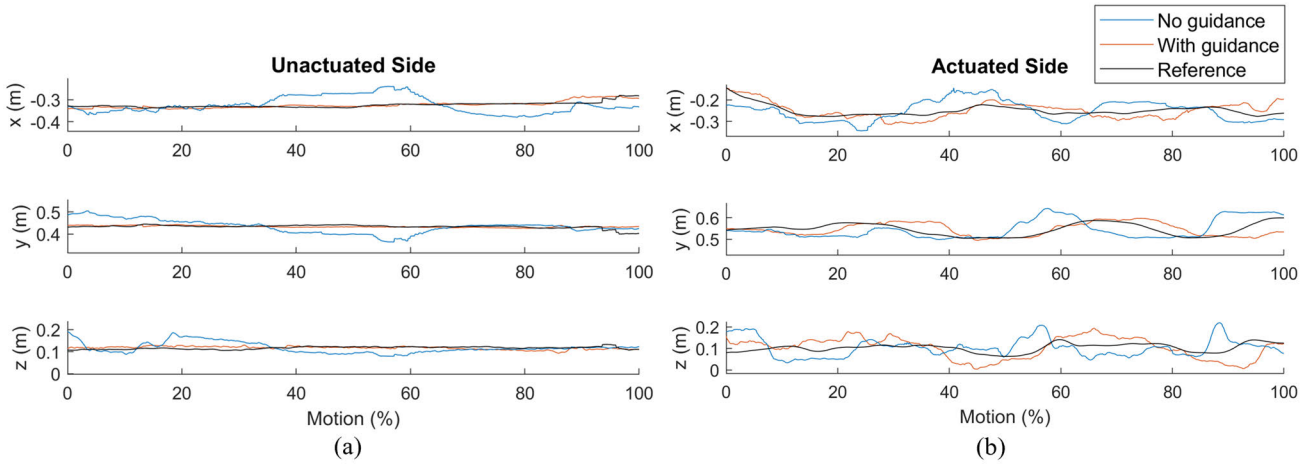

FIGURE 11. Subject J's (a) left and (b) right virtual hand position in the last trial with and without visual guidance, in the steak-cutting motion under transparent mode.

guidance can guide subjects to perform task- and joint-space movement. Note that the virtual hand position was computed with FK in Unity3D, relative to the base frame of VR, i.e., the base frame of UULE ($[x_0\ y_0\ z_0]$ in Fig. 1(c)).

So, this experimental result demonstrates the potential to verify the hypothesis that the guiding arm guided subjects with motion periods similar to reference motion and statistically significant reductions in angle errors of sF/E-A and wF/E-A. Such visual guidance is promising in guiding subjects to coordinate their unassisted and assisted joints. They can deliberately synchronize their unassisted joints to align with the motions of other assisted joints, focusing on timing and joint angles in particular. Although experimental results show a less prominent guiding effect on joint motion patterns, visual guidance is necessary to let subjects know the timing of every joint. They can anticipate the robot motion of assisted joints and coordinate their unassisted joints to match the assisted joint motion.

Next, Experiment 2 shows that the proposed framework can assist subjects' joints separately and simultaneously in an asymmetric bimanual ADL task with visual guidance. During the experiment, subjects performed a VR steak-cutting task in three operating modes with visual guidance: transparent mode (no assistance), elbow assistance mode, and arm assistance mode.

As shown in Fig. 12 and Fig. 13, the effect of assistance can be observed in subject J. Subject J's virtual hand positions are shown in Fig. 12, describing the task-space trajectories for both hands in the ADL task. Throughout the ADL task, subject J could perform complementary bilateral movements and activate the visual guidance and robot assistance by maintaining his/her left-hand position. In Fig. 13, the tendency of EMG signals matches joint movement in both transparent and two assistance modes; no adverse effects on muscle activities and joint movements are noticed in both assistance modes. Moreover, the reduced EMG signal can be observed in both assistance modes: Biceps(BIC) and Triceps (TRI) in elbow assistance mode, and most muscles in arm assistance, particularly the Anterior deltoid (DELA), Pronator teres (PTER) and Flexor carpi radialis (FCR). This indicates that subject J could activate and follow visual guidance, as well as use less muscle effort when UULE assisted his/her joints.

Furthermore, the angle errors were reduced at the assisted joint, especially eR-A in arm assistance mode (Fig. 13(c)). As mentioned, the visual guidance may not be sufficient to guide subjects at eR-A; hence, its robot assistance can be shown with reduced angle errors. RMS angle errors are 52.9° and 40.0° without robot assistance (transparent and elbow assistance modes), while RMS error is 8.9° in arm assistance mode. Hence, the reduced angle errors indicate the robot's assistance in ADL training.

The experimental analysis with 15 subjects shows a consistent assistance effect among subjects regarding EMG signals and angle error reduction. For example, the elbow assistance mode can show individual joint assistance. Fig. 14(a) shows a statistically significant EMG signal reduction ($p \leq 0.001$) in Biceps (BIC) and Triceps (TRI) with a one-tailed Wilcoxon signed rank test, and TABLE 3 shows the average EMG reduction up to 13.1% and 24.2%. Also, Fig. 14(b) and TABLE 4 present the statistically significant reduction ($p \leq 0.001$) of average RMS angle errors up to 41.6% at eF/E-A. Besides, all subjects can coordinate unassisted and assisted joints with elbow assistance to complete the task without adversely affecting other muscle activities and joint movements. This verifies that the proposed framework can assist subjects' specific joints in an asymmetric bimanual ADL task.

Although a reduction of EMG signal in Pronator teres (PTER) and Flexor carpi radialis (FCR) can also be observed in elbow assistance mode in Fig. 13 and Fig. 14, the angle errors at eR-A and wF/E-A have no statistically significant reduction ($p > 0.2$) to the transparent mode and are much larger than that in the arm assistance mode. These EMG reductions may be attributed to the robot weight

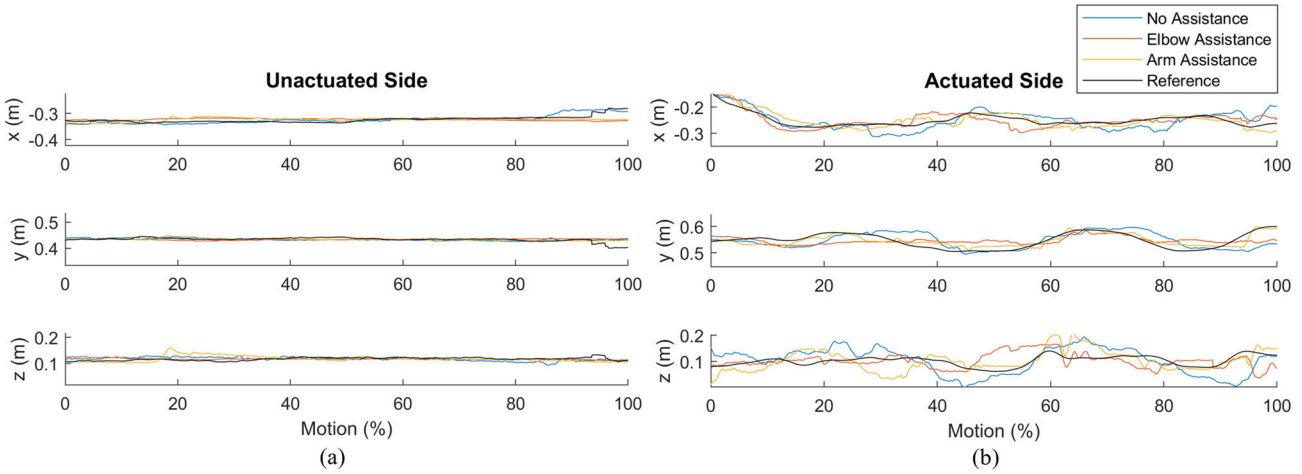

FIGURE 12. Subject J's virtual hand position on (a) the left unactuated side and (b) the right actuated side in last trial with visual guidance.

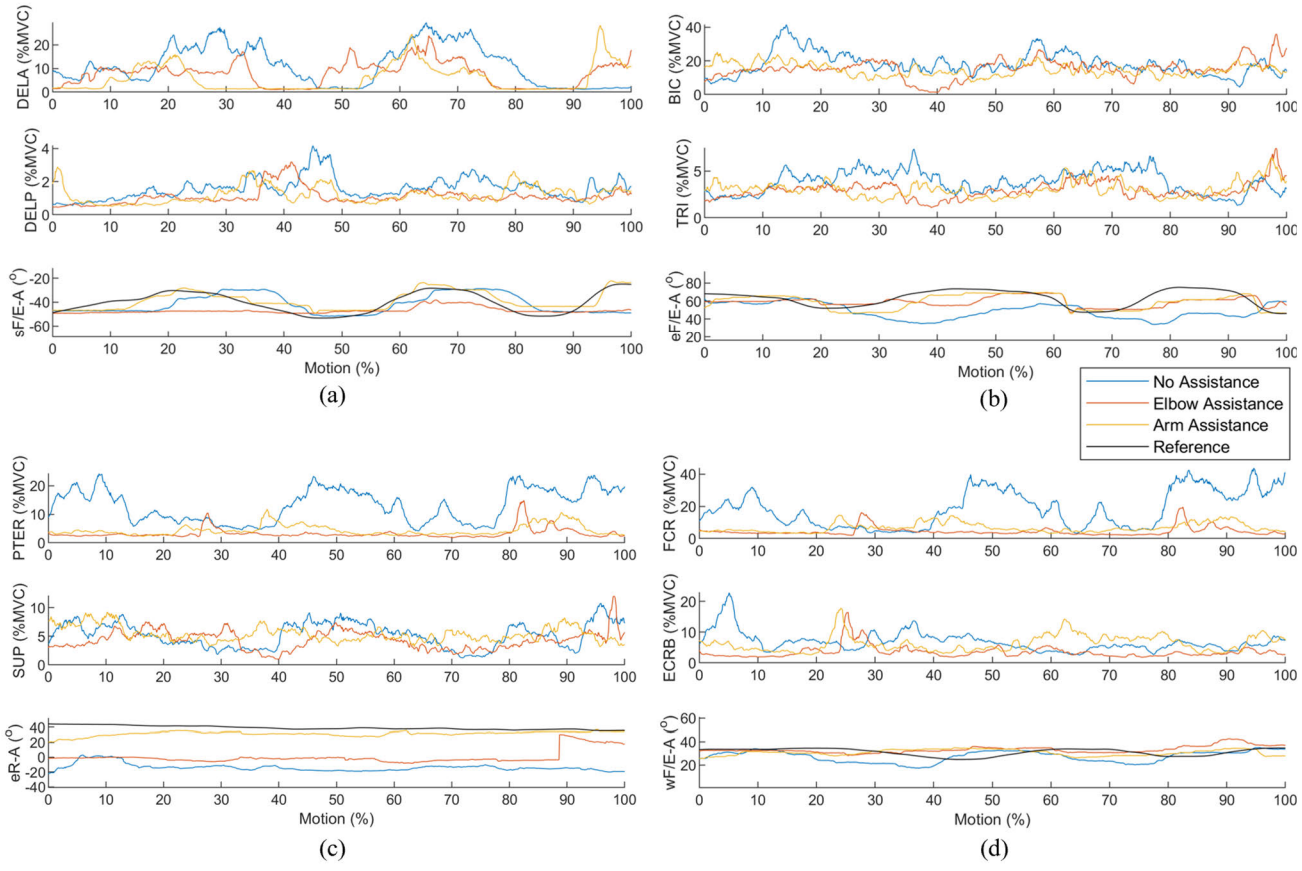

FIGURE 13. EMG signals and joint angles of subject J's right arm in last trial with visual guidance: (a) shoulder, (b) elbow, (c) forearm, and (d) wrist.

compensation algorithm at eF/E-A. After compensating the robot weight from eF/E-A to wF/E-A, subjects could move their forearm with lesser muscle effort. So, in terms of motion correction, the elbow assistance mode cannot assist subjects' joints other than their elbow.

In addition, the arm assistance mode shows robot assistance at multiple joints during ADL. Fig. 14(d) shows a statistically significant EMG reduction in all eight muscles in the arm assistance mode, particularly the Posterior Deltoid (DELP), Biceps (BIC), Pronator teres (PTER), and Flexor carpi radialis (FCR). These four muscles have a statistically significant reduction ($p \leq 0.001$), ranging from 34.9% to 67.6% in TABLE 3. Also, Fig. 14(e) and TABLE 4 exhibit the statistically significant reduction ($p \leq 0.001$)

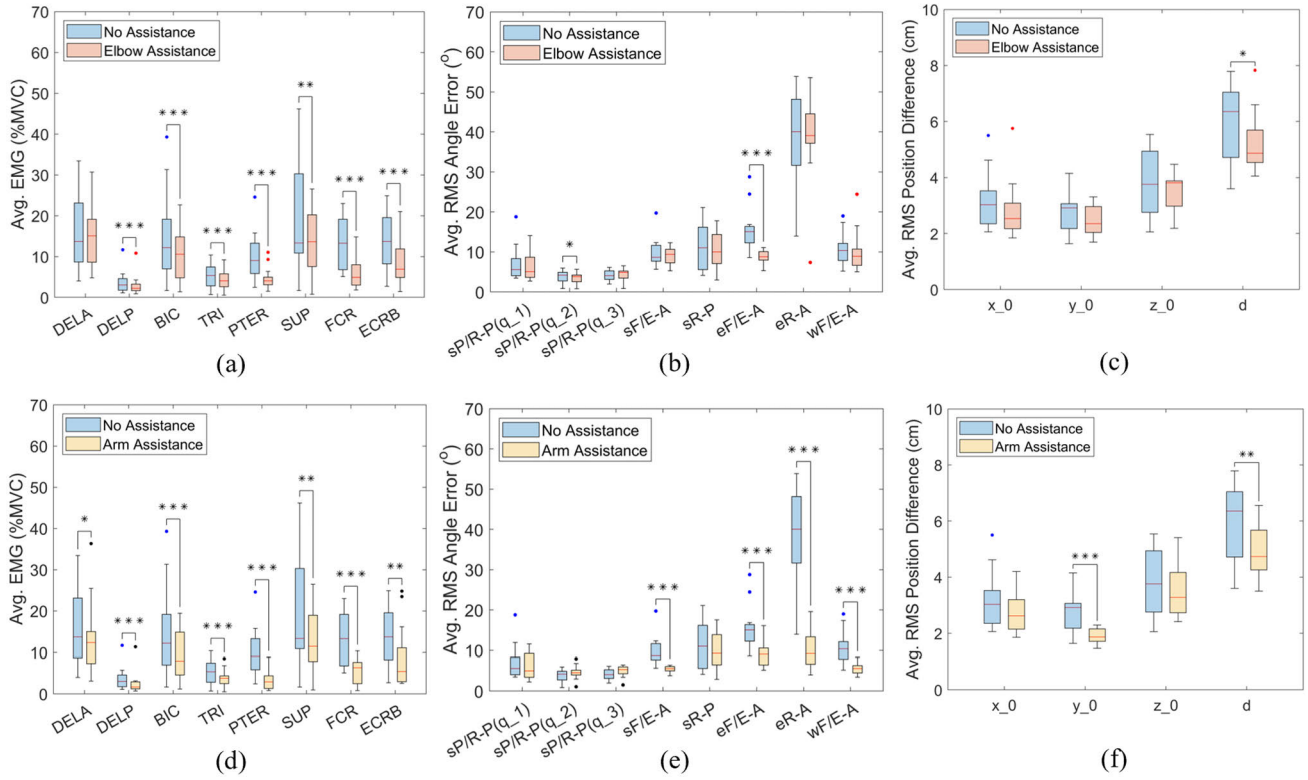

FIGURE 14. Given the visual guidance, (a, d) the average EMG signal across 15 subjects, (b, e) the average RMS joint angle error, and (c, f) average RMS position difference for right hand. The "d" represents Euclidean distance between the virtual hand and guiding hand, and the asterisks ('*,' '**,' '***') indicate statistical significance with $p \leq 0.05$, $p \leq 0.01$, and $p \leq 0.001$ in one-tailed Wilcoxon signed rank test.

TABLE 3. Percentage change of the median of avg. EMG signals compared to that without assistance.

	DELA	DELP	BIC	TRI	PTER	SUP	FCR	ECRB
With Elbow Assistance (%)	+10.0	-26.8	-13.1	-24.2	-55.0	+2.3	-63.0	-49.6
With Arm Assistance (%)	-10.1	-44.6	-34.9	-29.6	-67.6	-14.2	-52.3	-60.4

TABLE 4. Percentage change of the median of avg. RMS angle difference of robot joints compared to that without assistance.

Robot Joint	sP/R-P (q_1)	sP/R-P (q_2)	sP/R-P (q_3)	sF/E-A	sR-P	eF/E-A	eR-A	wF/E-A
With Elbow Assistance (%)	-9.2	-9.1	+19.9	+8.5	-9.3	-41.6	-2.4	-14.0
With Arm Assistance (%)	-10.4	+7.6	+30.2	-35.9	-15.9	-39.9	-77.0	-46.0

TABLE 5. Percentage change of median of avg. RMS position difference of virtual and guiding hand compared to that without assistance.

	x	y	z	d
With Elbow Assistance (%)	-16.3	-19.3	+1.5	-23.5
With Arm Assistance (%)	-13.6	-35.9	-12.7	-25.5

of average RMS angle errors at robot-assisted joints (sF/E-A, eF/E-A, eR-A, wF/E-A), ranging from 35.9% to 77.0%. This verifies that the proposed framework can assist multiple joints simultaneously in an asymmetric bimanual ADL task.

Although the proposed framework and underactuated UULE are not designed to track the task-space (hand) trajectory, Fig. 14(c, f) and TABLE 5 indicate the effect of joint assistance with a statistically significant reduction of 23.5% and 25.5% in Euclidean distance (d) between virtual and guiding hand position in elbow ($p \leq 0.05$) and arm assistance mode ($p \leq 0.01$), respectively. Additionally, the Euclidean distance maintains a slight average RMS difference (< 7.8 cm) in all three conditions, meaning that the accumulated joint angle error and the underactuated mechanism did not affect the hand trajectory much. Subjects

can coordinate the assisted and unassisted joints during ADL tasks.

Since the unassisted and passive joints cannot assist subjects, the joint angle errors of these joints may be increased in the assistance mode. As shown in Fig. 14(b, e), it shows the increased averaged angle error at sP/R-P (q_3)(0.8°) and sF/E-A (0.7°) in elbow assistance mode, as well as at sP/R-P (q_2, q_3) (0.3° and 1.2°, respectively) in arm assistance mode. This is attributed to different motion patterns during the ADL task. Because of human arm redundancy, subjects could have different intralimb coordination to complete the ADL task.

To sum up, Experiment 1 demonstrates the potential effect of the guiding arm with a motion period similar to reference ADL motions and the statistically significant reductions in angle errors of sF/E-A and wF/E-A. The statistically significant reductions in EMG signals and angle errors in Experiment 2 show that the proposed control framework with independent joint control and visual guidance assists subjects in an asymmetric bimanual ADL task. This result implies that subjects can coordinate unassisted and assisted joints during ADL, even with an underactuated exoskeleton like UULE. Hence, the proposed control framework can potentially assist stroke patients in asymmetric bimanual ADL training.

V. DISCUSSION

Today, robotic rehabilitation training for asymmetric bimanual ADL is often overlooked but necessary for stroke patients to regain ADL-related functions. Most robotic training focuses on symmetric motion, insufficient to relearn asymmetric bimanual ADL functions. Yet, the existing exoskeleton controls for such ADL focus on task space assistance. This may not be suitable for rehabilitation due to insufficient motion error for motor learning, difficulty setting joint trajectories and constraints in ADL, and difficulty adjusting robot assistance for individual joints.

To solve those challenges, this paper proposes a novel control framework with independent joint control and visual guidance in VR. With the therapist's demonstration, the joint trajectories for the robot joint controller and visual guidance can be set, solving the technical challenges of joint trajectory planning in ADL. Furthermore, assisting with independent joint impedance control allows therapists to adjust the assistance for individual joints according to patients' impairment and the tolerated joint error for motor learning. Also, training the ADL in VR can guarantee patients' safety even when they fail the ADL task. However, the concern of this approach was that the preset joint trajectory might not be intuitive to patients, leading to the coordination issue between assisted and unassisted joints. Patients may not know the robot's motion, let alone coordinate with their joint motions. Thus, VR visual guidance in the proposed framework helps address this concern.

Experiment 1 shows the potential that the guiding arm as visual guidance could guide subjects to complete the steak-cutting task with a motion period similar to reference ADL motion and statistically significant motion error reduction at sF/E-A and wF/E-A. Experiment 2 shows that the proposed framework with independent joint control and visual guidance in VR can assist subjects' joints separately or simultaneously in an asymmetric bimanual ADL task, with statistically significant reductions in EMG and angle errors at robot-assisted joints. As a result, we verified that subjects could understand the robot's motion and coordinate their unassisted and assisted joints during ADL. The proposed control framework can potentially assist stroke patients in asymmetric bimanual ADL training.

Furthermore, this bimanual VR task can train interlimb coordination and guarantee bimanual motion during ADL training. Fig. 11 shows that subject J's left hand was more stable in the with-guidance condition than in the no-guidance condition. Due to neural crosstalk [7], [34], the right arm's movement may affect the left arm's; hence, subjects' left hand may not stay constant and maintain the desired interlimb coordination during bilateral complementary motion. Fig. 11 verifies that this bimanual VR task can ensure subjects perform bilateral complementary motion since the right guiding arm was provided only when the red target was disabled by their left hand. Hence, this feature for visual guidance activation can train interlimb coordination and guarantee bimanual motion during ADL training.

Another observation from experimental results is related to the joint trajectory planning issue with different body dimensions. Since the experiments were conducted with 15 subjects with different body dimensions, the consistent experimental result suggests that the proposed framework focusing on joint space can be used for patients with various arm lengths with the same virtual arm lengths in VR. Also, the result shows that 15 subjects were assisted in ADL with the author's pre-recorded joint trajectories. It implies that occupational therapists may teach patients compensatory techniques involving specific joint movements through the proposed framework, even though they have different body dimensions.

While our study utilized a VR steak-cutting task to evaluate the proposed control framework, it is crucial to acknowledge certain experiment limitations. The VR task employed in this proof-of-concept was purely kinematic, lacking interactions with the environment. Given that this paper is our inaugural exploration of the proposed framework, we deliberately chose a simplified VR steak-cutting task to minimize the potential risks in human experiments, excluding physical environmental constraints and interactions involving surrounding objects such as tables and steaks. Although this simplification may impact the training experience for patients and the transferability of acquired skills to real-world tasks, it represents a foundational step in validating our proposed control framework. Future works should investigate more realistic VR tasks involving environmental interactions to generalize our findings.

Furthermore, an aspect not thoroughly addressed in this paper is the distinction between visual cues in task space (i.e., the colored targets for the knife in Fig. 4) and joint

space (i.e., the guiding arm). The current investigation integrated these visual cues to validate the proposed framework, but a direct comparison was not undertaken between these two forms of visual cues. Thus, the individual impacts of task-space and joint-space visual cues on human subjects remain unclear. Future works should examine the effects of task-space and joint-space visual cues separately to understand their guiding effect, inspiring us to design the most suitable method for stroke rehabilitation.

Regarding research significance, the proposed control framework benefits various exoskeleton designs since it independently controls the active joints' movement. For example, redundantly-actuated exoskeletons like Harmony [18], ARMin [19], CURER [34], and NESM$-\gamma$ [35]; underactuated exoskeletons with passive joints like UULE [24], ASSISTON-SE [20], and NESM [21]; and wearable exoskeletons with fewer DoFs like Elbow-Wrist Exoskeleton [36] and portable shoulder exoskeleton [37]. Also, it is not required to have any specific and complicated controller for different kinds of exoskeletons. This can potentially be used with other existing exoskeleton controllers concurrently. Furthermore, such a joint-space control framework can simultaneously control multiple separated exoskeleton devices for various joints during ADL training, according to the needs of patients.

Furthermore, the framework can train not only the asymmetric bimanual motion but also the unimanual motion. Since robotic unimanual ADL training suffers similar technical challenges in joint trajectory planning for patient assistance, the individual joint assistance and visual guidance recorded by therapists can also be suitable for unimanual ADL training.

VI. CONCLUSION

This paper presents a novel control framework for asymmetric bimanual ADL training, incorporating independent joint control and visual guidance. The framework contributes to rehabilitation robotics in three key ways:

1) We provide individual assistance for impaired joints through joint-space control, which differs from traditional task-space control. This is substantiated by the statistically significant reduction in muscle activities and elbow angle error (eF/E-A) during the 15-healthy-subject experiment with elbow assistance mode. This approach addresses a crucial limitation in current methodologies with task-space control.
2) Employing the same virtual arm in virtual reality (VR) to record and teach human-demonstrated ADL motions resolves challenges associated with joint reference trajectories. The experiment supports this with statistically significant reductions in muscle activities and angle errors at the robot-assisted joints. This effect is observed in 15 healthy subjects with varying arm dimensions, all guided by author-demonstrated joint trajectories. This approach holds promise for tailored compensatory techniques in occupational therapy.
3) The real-time VR visual guidance is crucial in helping subjects synchronize their movements with the human-demonstrated motions. It aids subjects in anticipating robot assistance from active joints and self-correcting their unassisted joint motion, thereby enhancing coordination between unassisted and assisted joints. The experiment validates the efficacy of visual guidance, demonstrating motion periods similar to the reference ADL motion and statistically significant angle error reduction at sF/E-A and wF/E-A. The experiment on robot assistance further supports this, revealing statistically significant reductions in muscle activities and angle errors at the robot-assisted joints. This approach shows potential for application in stroke patient interventions.

The proposed control framework offers an alternative approach to robotic rehabilitation, diverging from traditional task-space control methods. To ascertain its effectiveness in rehabilitation training, further clinical validation involving chronic stroke patients is imperative.

REFERENCES

[1] H. Rodgers, "Robot assisted training for the upper limb after stroke (RATULS): A multicentre randomised controlled trial," *Lancet*, vol. 394, no. 10192, pp. 51–62, Jul. 2019.
[2] H. Nakayama, H. Stig Jørgensen, H. Otto Raaschou, and T. Skyhøjolsen, "Recovery of upper extremity function in stroke patients: The Copenhagen stroke study," *Arch. Phys. Med. Rehabil.*, vol. 75, no. 4, pp. 394–398, Apr. 1994.
[3] C. Xu, S. Li, K. Wang, Z. Hou, and N. Yu, "Quantitative assessment of paretic limb dexterity and interlimb coordination during bilateral arm rehabilitation training," in *Proc. Int. Conf. Rehabil. Robot. (ICORR)*, Jul. 2017, pp. 634–639.
[4] H. M. Qassim and W. Z. W. Hasan, "A review on upper limb rehabilitation robots," *Appl. Sci.*, vol. 10, no. 19, p. 6976, Oct. 2020.
[5] D. Kong, W. Wang, and Y. Shi, "Design of master-slave velocity tracking upper-limb exoskeleton system and feed-forward compensation control," Res. Square, Apr. 2021, doi: 10.21203/rs.3.rs-326570/v1.
[6] S. M. Waller and J. Whitall, "Bilateral arm training: Why and who benefits?" *NeuroRehabilitation*, vol. 23, no. 1, pp. 29–41, Mar. 2008.
[7] R. Sainburg, D. Good, and A. Przybyla, "Bilateral synergy: A framework for post-stroke rehabilitation," *J. Neurol. Transl. Neurosci.*, vol. 1, no. 3, p. 1025, 2013.
[8] L. A. Legg, S. R. Lewis, O. J. Schofield-Robinson, A. Drummond, and P. Langhorne, "Occupational therapy for adults with problems in activities of daily living after stroke," *Cochrane Database Systematic Rev.*, vol. 7, no. 7, Jul. 2017, Art. no. CD003585.
[9] T. Nef, M. Mihelj, and R. Riener, "ARMin: A robot for patient-cooperative arm therapy," *Med. Biol. Eng. Comput.*, vol. 45, no. 9, pp. 887–900, Sep. 2007.
[10] T. Nef, M. Mihelj, G. Kiefer, C. Perndl, R. Müller, and R. Riener, "ARMin–exoskeleton for arm therapy in stroke patients," in *Proc. IEEE 10th Int. Conf. Rehabil. Robot.*, Jun. 2007, pp. 68–74.
[11] M. Mihelj, T. Nef, and R. Riener, "A novel paradigm for patient-cooperative control of upper-limb rehabilitation robots," *Adv. Robot.*, vol. 21, no. 8, pp. 843–867, Jan. 2007.
[12] S. D. Gasperina, K. Ghonasgi, A. C. de Oliveira, M. Gandolla, A. Pedrocchi, and A. Deshpande, "A novel inverse kinematics method for upper-limb exoskeleton under joint coordination constraints," in *Proc. IEEE/RSJ Int. Conf. Intell. Robots Syst. (IROS)*, Oct. 2020, pp. 3404–3409.
[13] M. Nann, F. Cordella, E. Trigili, C. Lauretti, M. Bravi, S. Miccinilli, J. M. Catalan, F. J. Badesa, S. Crea, F. Bressi, N. Garcia-Aracil, N. Vitiello, L. Zollo, and S. R. Soekadar, "Restoring activities of daily living using an EEG/EOG-controlled semiautonomous and mobile whole-arm exoskeleton in chronic stroke," *IEEE Syst. J.*, vol. 15, no. 2, pp. 2314–2321, Jun. 2021.

[14] M. Gandolla, S. D. Gasperina, V. Longatelli, A. Manti, L. Aquilante, M. G. D'Angelo, E. Biffi, E. Diella, F. Molteni, M. Rossini, M. Gföhler, M. Puchinger, M. Bocciolone, F. Braghin, and A. Pedrocchi, "An assistive upper-limb exoskeleton controlled by multi-modal interfaces for severely impaired patients: Development and experimental assessment," *Robot. Auto. Syst.*, vol. 143, Sep. 2021, Art. no. 103822.
[15] T. Kitago and J. W. Krakauer, "Motor learning principles for neurorehabilitation," in *Handbook of Clinical Neurology*, vol. 110, M. P. Barnes and D. C. Good, Eds. Amsterdam, The Netherlands: Elsevier, 2013, pp. 93–103.
[16] R. Iandolo, F. Marini, M. Semprini, M. Laffranchi, M. Mugnosso, A. Cherif, L. De Michieli, M. Chiappalone, and J. Zenzeri, "Perspectives and challenges in robotic neurorehabilitation," *Appl. Sci.*, vol. 9, no. 15, p. 3183, Aug. 2019.
[17] E. Burdet, D. Franklin, and T. Milner, *Human Robotics: Neuromechanics and Motor Control*. Cambridge, MA, USA: MIT Press, May 2018.
[18] B. Kim and A. D. Deshpande, "An upper-body rehabilitation exoskeleton harmony with an anatomical shoulder mechanism: Design, modeling, control, and performance evaluation," *Int. J. Robot. Res.*, vol. 36, no. 4, pp. 414–435, Apr. 2017.
[19] T. Nef, M. Guidali, and R. Riener, "ARMin III–Arm therapy exoskeleton with an ergonomic shoulder actuation," *Appl. Bionics Biomechanics*, vol. 6, Jan. 2009, Art. no. 962956.
[20] M. A. Ergin and V. Patoglu, "ASSISTON-SE: A self-aligning shoulder-elbow exoskeleton," in *Proc. IEEE Int. Conf. Robot. Autom.*, May 2012, pp. 2479–2485.
[21] E. Trigili, S. Crea, M. Moisè, A. Baldoni, M. Cempini, G. Ercolini, D. Marconi, F. Posteraro, M. C. Carrozza, and N. Vitiello, "Design and experimental characterization of a shoulder-elbow exoskeleton with compliant joints for post-stroke rehabilitation," *IEEE/ASME Trans. Mechatronics*, vol. 24, no. 4, pp. 1485–1496, Aug. 2019.
[22] S. Y. A. Mounis, N. Z. Azlan, and F. Sado, "Assist-as-needed control strategy for upper-limb rehabilitation based on subject's functional ability," *Meas. Control*, vol. 52, nos. 9–10, pp. 1354–1361, Nov. 2019.
[23] E. T. Wolbrecht, V. Chan, D. J. Reinkensmeyer, and J. E. Bobrow, "Optimizing compliant, model-based robotic assistance to promote neurorehabilitation," *IEEE Trans. Neural Syst. Rehabil. Eng.*, vol. 16, no. 3, pp. 286–297, Jun. 2008.
[24] T. M. Kwok, T. Li, and H. Yu, "A reliable kinematic measurement of upper limb exoskeleton for VR therapy with visual-inertial sensors," in *Proc. IEEE/ASME Int. Conf. Adv. Intell. Mechatronics (AIM)*, Jun. 2023, pp. 584–590.
[25] X.-L. Hu, R. K.-Y. Tong, N. S. K. Ho, J.-J. Xue, W. Rong, and L. S. W. Li, "Wrist rehabilitation assisted by an electromyography-driven neuromuscular electrical stimulation robot after stroke," *Neurorehabilitation Neural Repair*, vol. 29, no. 8, pp. 767–776, Sep. 2015.
[26] J. C. Perry, J. Rosen, and S. Burns, "Upper-limb powered exoskeleton design," *IEEE/ASME Trans. Mechatronics*, vol. 12, no. 4, pp. 408–417, Aug. 2007.
[27] T. L. Brooks, "Telerobotic response requirements," in *Proc. IEEE Int. Conf. Syst. Man, Cybern. Conf.*, Nov. 1990, pp. 113–120.
[28] J. H. Cauraugh and J. J. Summers, "Neural plasticity and bilateral movements: A rehabilitation approach for chronic stroke," *Prog. Neurobiol.*, vol. 75, no. 5, pp. 309–320, Apr. 2005.
[29] K. s. Fu, R. C. Gonzalez, and C. S. G. Lee, *Robotics: Control, Sensing, Vision*. New York, NY, USA: McGraw-Hill, 1987.
[30] M. Pyasik, G. Tieri, and L. Pia, "Visual appearance of the virtual hand affects embodiment in the virtual hand illusion," *Sci. Rep.*, vol. 10, no. 1, p. 5412, Mar. 2020.
[31] S. Seinfeld and J. Müller, "Impact of visuomotor feedback on the embodiment of virtual hands detached from the body," *Sci. Rep.*, vol. 10, no. 1, p. 22427, Dec. 2020.
[32] P.-W. Chen, N. A. Baune, I. Zwir, J. Wang, V. Swamidass, and A. W. K. Wong, "Measuring activities of daily living in stroke patients with motion machine learning algorithms: A pilot study," *Int. J. Environ. Res. Public Health*, vol. 18, no. 4, p. 1634, Feb. 2021.
[33] N. Wenk, J. Penalver-Andres, R. Palma, K. A. Buetler, R. Müri, T. Nef, and L. Marchal-Crespo, "Reaching in several realities: Motor and cognitive benefits of different visualization technologies," in *Proc. IEEE 16th Int. Conf. Rehabil. Robot. (ICORR)*, Jun. 2019, pp. 1037–1042.
[34] W. Qian, J. Liao, L. Lu, L. Ai, M. Li, X. Xiao, and Z. Guo, "CURER: A lightweight cable-driven compliant upper limb rehabilitation exoskeleton robot," *IEEE/ASME Trans. Mechatronics*, vol. 28, no. 3, pp. 1730–1741, Nov. 2022.
[35] J. Pan, D. Astarita, A. Baldoni, F. Dell'Agnello, S. Crea, N. Vitiello, and E. Trigili, "NESM-: An upper-limb exoskeleton with compliant actuators for clinical deployment," *IEEE Robot. Autom. Lett.*, vol. 7, no. 3, pp. 7708–7715, Jul. 2022.
[36] K.-Y. Wu, Y.-Y. Su, Y.-L. Yu, C.-H. Lin, and C.-C. Lan, "A 5-degrees-of-freedom lightweight elbow-wrist exoskeleton for forearm fine-motion rehabilitation," *IEEE/ASME Trans. Mechatronics*, vol. 24, no. 6, pp. 2684–2695, Dec. 2019.
[37] L. Tiseni, M. Xiloyannis, D. Chiaradia, N. Lotti, M. Solazzi, H. van der Kooij, A. Frisoli, and L. Masia, "On the edge between soft and rigid: An assistive shoulder exoskeleton with hyper-redundant kinematics," in *Proc. IEEE 16th Int. Conf. Rehabil. Robot. (ICORR)*, Jun. 2019, pp. 618–624.

THOMAS M. KWOK (Member, IEEE) received the B.Eng. and M.Phil. degrees in mechanical and automation engineering from The Chinese University of Hong Kong, Hong Kong SAR, China, in 2016 and 2019, respectively, and the Ph.D. degree from the Integrative Sciences and Engineering Program, NUS Graduate School, National University of Singapore, Singapore, in 2023.

His research interests include robot design and control, rehabilitation engineering, and physical human–robot interaction.

HAOYONG YU (Senior Member, IEEE) received the B.S. and M.S. degrees in mechanical engineering from Shanghai Jiao Tong University, Shanghai, China, in 1988 and 1991, respectively, and the Ph.D. degree in mechanical engineering from the Massachusetts Institute of Technology, Cambridge, MA, USA, in 2002.

He is currently an Associate Professor with the Department of Biomedical Engineering, National University of Singapore, Singapore. His research interests include medical robotics, rehabilitation engineering and assistive technologies, system dynamics, and control.